Physics Open 5 (2020) 100036

Contents lists available at ScienceDirect

Physics Open

journal homepage: www.journals.elsevier.com/physics-open

BoCXS: A compact multidisciplinary X-ray source

A. Bazzani [a], P. Cardarelli [b], G. Paternò [b,c], M. Placidi [d,*], A. Taibi [b,c], G. Turchetti [a]

[a] Dipartimento di Fisica e Astronomia, Università di Bologna, Via Irnerio 46, 40126, Bologna, Italy
[b] INFN-Sez. Ferrara, Via G. Saragat 1, 44122, Ferrara, Italy
[c] Dipartimento Fisica e Scienze Della Terra, Università di Ferrara, Via G. Saragat 1, 44122, Ferrara, Italy
[d] Guest at Lawrence Berkeley National Laboratory, Berkeley, CA 94720, USA

ARTICLE INFO

Handling editor: William Barletta

Keywords:
Lasers
Compton scattering
Optics
KES

ABSTRACT

Many research and application areas demand photon sources capable of producing quasi-monochromatic X-ray beams in the multi-keV energy range with reasonably high fluxes and compact footprints. Besides industrial, research, commercial and cultural heritage applications, various biomedical applications could benefit from the features of this type of X-ray sources. The main target of our proposal is the production of X-ray beams with energy range tunability, monochromaticity, flux and pulse duration, compatible with those required by various pre-clinical imaging modalities and material characterization techniques, through inverse Compton scattering. This kind of source involves an infrastructure much more compact than a large Synchrotron facility and can be realized on a laboratory scale enabling an easier access to a local community of users.

1. Introduction

X-rays are a fundamental probe to investigate the various properties of matter both for fundamental research and for several interdisciplinary applications.

Main characteristics of the radiation as photon energy, monochromaticity, intensity, spot size, pulse duration and brilliance play essential roles in the quality of the attainable information in the photon-matter interaction.

An important area of interest is represented by biomedical imaging. A variety of anatomical districts could be imaged with quasi-monochromatic X-ray beams maximizing the signal-to-noise ratio and reducing, at the same time, the adsorbed radiation dose. Furthermore, while dense materials containing significant fraction of heavy elements, such as bones, provide a sufficiently high contrast also with conventional photon source based on X-ray tubes, soft tissues are more challenging to be imaged. Indeed, they are often hidden by background anatomical structures in images obtained with conventional X-ray absorption techniques. In order to enhance the visibility of soft tissues, techniques like K-edge subtraction (KES) or phase contrast imaging (PCI) can be used. They require intense, tunable and monochromatic photon beams. Moreover, for PCI is mandatory a high level of coherence of the source. All these features can be easily obtained at large accelerator facilities.

Synchrotron-based light sources store multi-GeV electron beams and have them passing through magnetic insertion devices (undulators, wigglers). A 2 cm period undulator requires an electron beam with an energy of several GeV and a storage ring in the 60–300 m diameter range to produce radiation with the above characteristics. Synchrotron light sources are large national or international facilities simultaneously providing many user stations with brilliant X-rays beams in the multi-keV range at MHz frequencies. The important financial efforts involved both in their construction and operation spoil their availability to biomedical and other applications.

By contrast, thanks to a striking progress in laser technology in the past ten years, compact X-ray sources based on the inverse Compton scattering (ICS) process, where moderate-energy electrons interact with high-intensity laser pulses, represent promising innovative sources capable of producing intense, high-energy X-ray beams with characteristics comparable with those available at large synchrotron light sources at a fraction of their cost and dimensions about two orders of magnitude smaller.

The availability of energy-tunable, monochromatic X-ray beams produced through compact sources of moderate cost and limited space requirements, which can then be installed in clinics and university lab-

Given his role as Editor of this journal, M. Placidi had no involvement in the peer-review of articles for which he was an author and had no access to information regarding their peer-review. Full responsibility for the peer-review process for this article was delegated to another Editor.

* Corresponding author.
E-mail address: massimoplacidi@icloud.com (M. Placidi).

https://doi.org/10.1016/j.physo.2020.100036
Received 4 May 2020; Received in revised form 6 July 2020; Accepted 8 August 2020
Available online 27 August 2020

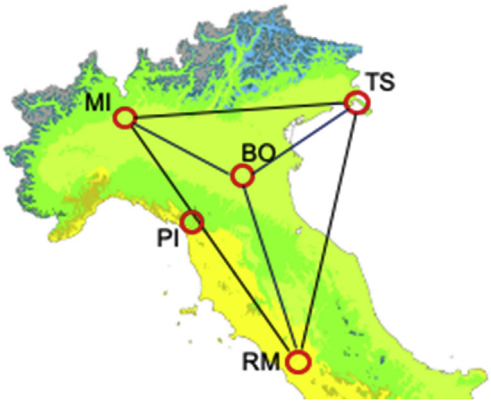

Fig. 1. A research triangle centered around the Bologna metropolitan area.

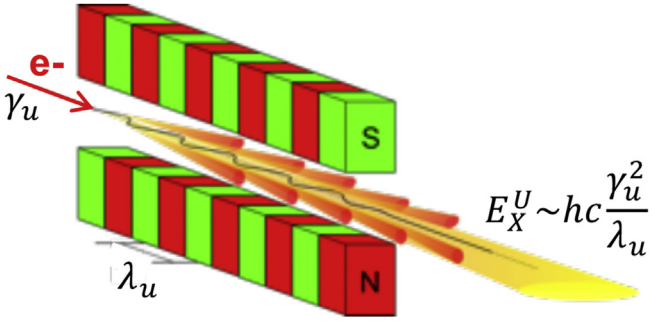

Fig. 2. Radiation from electrons passing through a Storage Ring Undulator.

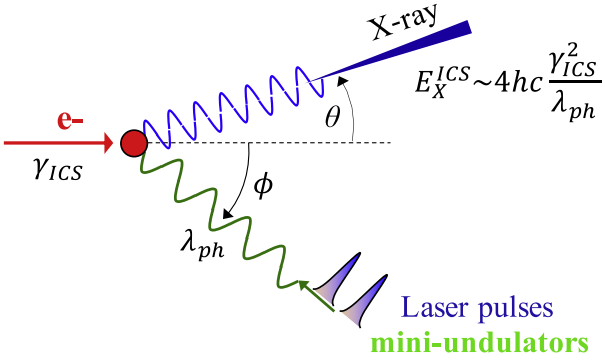

Fig. 3. Radiation from electrons interacting with laser pulses.

oratories, would boost a remarkable progress in the attainable quality of imaging information, enabling also the implementation of innovative analysis techniques. The possible applications made available by the multidisciplinary characteristics of an ICS-based compact X-ray source extend beyond advanced biomedical imaging, where $\leq$ 80 keV X-ray energies are the main target for preclinical research to clinical use. Basic research in condensed matter would benefit from the high spatial coherence and the short duration of the light pulses, typically in the ps range. Non-destructive tests for mechanical and automotive industry would be also available by rising the X-ray energy up to 1 MeV, as illustrated later. Cultural heritage science performed within this energy range could extend the applications of conventional sources, allowing the characterization of nature and composition of artifacts more complex in structure and size.

This document outlines a proposal aiming at designing, building, installing and operating an ICS-based compact X-ray source in the

Fig. 4. ESRF: 6 GeV electrons, 850 m circumference.

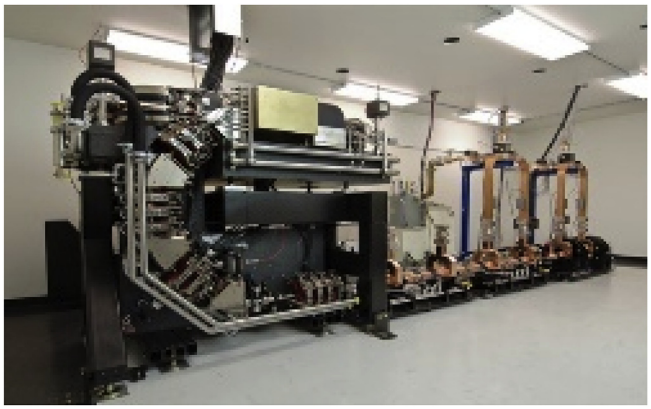

Fig. 5. CLS at LTI premises: 40 MeV electrons, 5×4 m^2 footprint.

Bologna metropolitan area, BoCXS (**Bo**logna **C**ompact **X**-ray **S**ource). The facility would be geographically located at the centre of a scientific triangle (Fig. 1) with a rich academic tradition where synergy possibilities with national scientific institutions would represent a precious option. It would moreover be strategically placed between larger scale facilities like Elettra and FERMI in Trieste and ESRF in Grenoble.

The proposal outlined here is based on the assumption that the availability of a compact source providing X-ray beams with characteristics of monochromaticity similar to those obtainable al large Synchrotron-based light sources, at a fraction of required space and cost and with a somehow easier accessibility, would represent a remarkable step in the direction of improving the imaging quality of emerging scientific applications. Although mainly conceived for applications in biomedical diagnostics, the wide range of possible applications in research and industry would confer to this facility a unique multidisciplinary character in Italy.

2. Accelerator-driven X-ray sources

Conventional X-ray sources are affordable, commercially available and their compactness makes them easy to transport and use but they miss some of the main characteristics of the radiation like monochromaticity, brightness and pulse duration which play essential roles in the photon-matter interaction and in the quality of the attainable information. These characteristics are available in accelerator-driven sources.

2.1. *Synchrotron light sources*

Synchrotron-based light sources are storage rings where electron beams traveling through magnetic Insertion Devices (undulators,

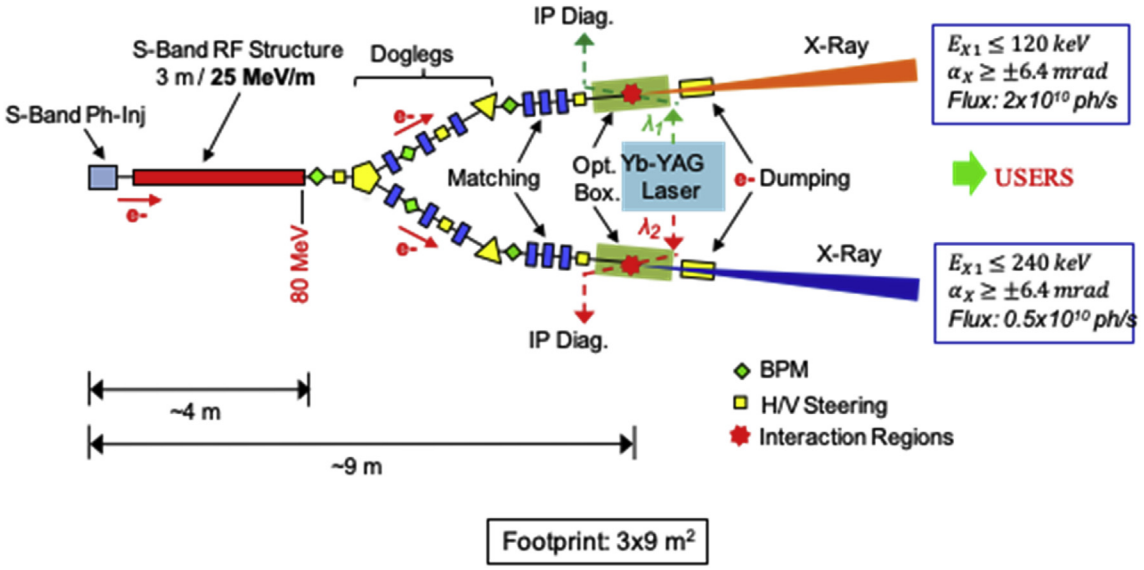

Fig. 6. The proposed BoCXS X-ray source in its base configuration. Electron bunches accelerated up to 80 MeV are transported to two optical interaction regions where they interact with intense photon pulses produced by the same laser system operating on the fundamental ($\lambda^0_{pk} = 1.03\mu m$) and its second harmonic. X-ray pulses are emitted along two arms in two different energy bands alternatively feeding user areas with different applications.

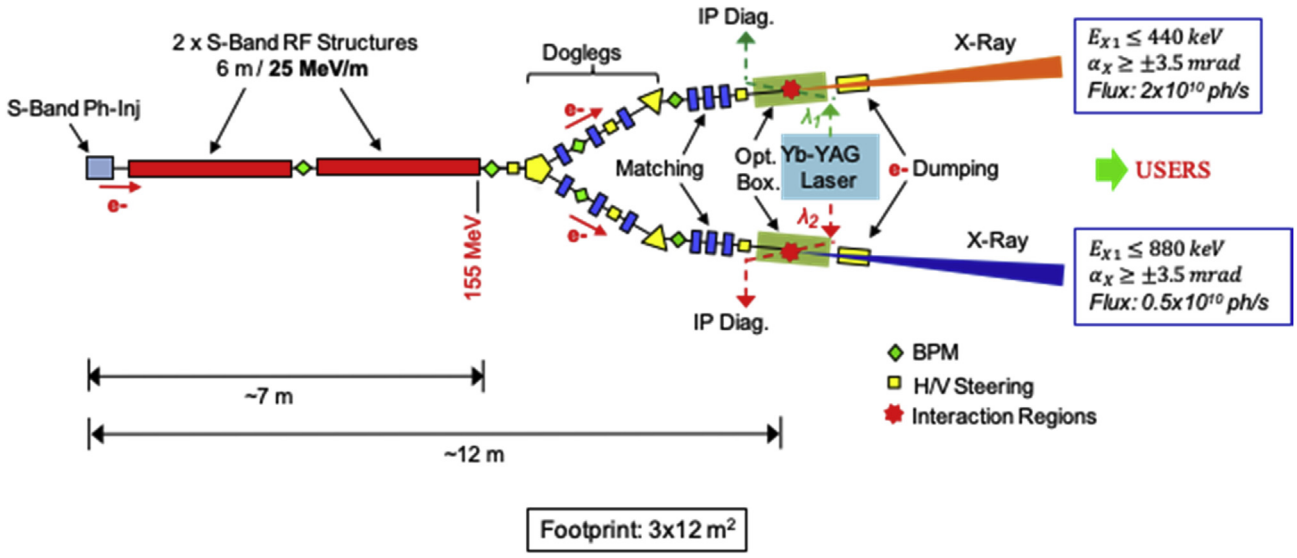

Fig. 7. BoCXS upgraded layout representing the most flexible version of the proposed source. The electron energy and the laser harmonic can be tuned to provide X-ray beams covering an energy range from below 100 keV to about 0.9 MeV.

wigglers) emit intense and bright X-ray beams at MHz frequencies (Fig. 2). A typical 15 mm period undulator requires a several GeV electron beam and a storage ring about 60–300 m in diameter to produce high brightness X-ray beams in the multi-keV energy range.

The on-axis undulator radiation wavelength is related to the longitudinal electron velocity β_z and the undulator period λ_u as [1].

$$\lambda_X^U = \lambda_u \frac{1-\beta_z}{\beta_z} \approx \left(\frac{1+\alpha_u^2}{2}\right)\frac{\lambda_u}{\gamma_u^2} \tag{1}$$

where γ_u is the Lorentz factor of the electron beam in the undulator and a_u is related to the undulator strength $K_u = eB_0\lambda_u/(2\pi\, m_e c) = 93.4\, B_0[T]\, \lambda_u[m]$ with B_0 the undulator central magnetic field, e and m_e the electron charge and rest mass and c the speed of light. In particular, $a_u = K_u$ for a helical undulator while for a planar-polarized undulator $a_u = K_u/\sqrt{2}$. For typical design parameters ($B_0 = 1T,\ \lambda_u = 15\ mm$) the quantity in parenthesis in (1) lies between 1 and 1.5 and the emitted photons energy has the parametric expression

$$E_X^U \equiv \frac{hc}{\lambda_X^U} \sim hc\,\frac{\gamma_u^2}{\lambda_u} \tag{2}$$

where $h = 6.626\ 10^{-34}\ J\ s$ is the Planck constant.

2.2. ICS-based light sources

ICS-based Light Sources accomplish the same task with lower fluxes but more compact, cost-effective and accessible installations. In the "wave nature" framework, electrons interact with the electromagnetic field associated to counter-traveling photons the same way as when passing through the alternating-polarity field of an undulator and create a radiation spectrum similar to that emitted in an undulator. In a classical

Table 1
BoCXS expected performance in Base (I) and Upgraded configuration (II).

SOURCE	Parameter	Symbol	Units	OPERATIONAL PHASE	
				I	*II*
ALL	Energy	E_e	*MeV*	80	155
S-BAND	Bunch charge	Q	*pC*	500	500
Linac	Bunch length	τ_b	*ps*	3.5	3.5
	Rep. Rate	r_e	*Hz*	100	100
	Peak Current	I_p	*A*	143	143
	Average Current	$<I_L>$	*μA*	0.050	0.050
	Beam Power	P_b	*W*	4.0	7.75
	Duty Cycle	D	-	3.5×10^{-10}	3.5×10^{-10}
Yb-YAG	Pulse energy	E_L^0	*J*	0.85	0.85
Laser	Wavelength	λ	*nm*	1030–515	1030–515
	Harmonic	h_L	-	1–2	1–2
	Pulse length	τ_{ph}	*ps*	5	5
	Rep. Rate	r_L	*Hz*	100	100
Interaction	e− Norm.	$\varepsilon_{x,y}^0$	*μm*	2.5/1.5	2.5/1.5
Region	Emittance				
	e− Energy spread	δ_E	%	0.2	0.2
	e− spot size, rms	$\sigma_{x,y}^*$	*μm*	15/10	15/10
	Interaction angle	ϕ	*deg*	2–10	2–10
	Laser waist, rms	w_0	*μm*	25	25
X-ray	Energy	E_X	*keV*	≤120–240	≤440–880
	Pulse duration	τ_X	*ps*	<5	<5
	Divergence, rms	σ_X'	*mrad*	≤ ±6	≤ ±2
	Intensity	$\dot{N}_X$	*ph/s*	(2.0–0.5) x10^{10}	
	Brightness		*$*	10^{11}–10^{12}	

$: Ph/s/mm^2/mrad^2/0.1%BW.

ICS approach (particle light nature) [2–7] a relativistic electron transfers a fraction of its energy to a counterpropagating photon (Fig. 3). The energy of the back-scattered radiation

Table 2
Optical scheme parameters.

Symbol	Size	Description
$\Delta\phi_1$	2° – 10°	Operational ϕrange
$\Delta\phi_2$	20° – 35°	Dual energy ϕrange
$f_{1,2}$	315.0/210.0 mm	OAPs focal length
A_{IR}	±10 mm	Clearance to e−/X beams
p	1 mm	Laser-mirror margin
M_1	~20.0 mm	Scanning mirror
$M_{2,3,4,5,6}$	~64.0 mm	Driving mirrors
$OAP_{1,2,3,4}$	~45.0 mm	Focusing mirrors
W_{opt}/L_{opt}	~340/670 mm^2	Opt. Box width/length

$$E_X^{ICS} = \alpha_c\, E_{ph}\, \gamma_{ICS}^2 = hc\, \alpha_c \frac{\gamma_{ICS}^2}{\lambda_{ph}} \tag{3}$$

results from a γ_{ICS}^2 boost from the electron to the incoming photon energy E_{ph}, associated to a relativistic Doppler shift of its wavelength λ_{ph}

$$\lambda_X^{ICS} = \frac{1}{\alpha_c}\frac{\lambda_{ph}}{\gamma_{ICS}^2}. \tag{4}$$

The kinematic factor

$$\alpha_c = \frac{2(1+cos\phi)}{1+\xi+(\gamma\theta)^2} < 4 \tag{5}$$

describes the dependence of the scattered energy on the collision angle ϕ and the scattering angle θ and accounts for the electron recoil in the ICS process via the term

$$\xi = 2\gamma_{ICS}^2 \frac{E_{ph}}{E_{ICS}}(1+cos\phi) \tag{6}$$

where E_{ICS}, γ_{ICS} are the energy and the Lorentz factor of the electron beam. The term (6) introduces a red-shift in the spectra of the emitted radiation and can have not negligible effects in terms of required radiation bandwidth. With the energies at play in our case it is of the order of 5×10^{-3} and can be neglected in the following considerations so the expression (3) simplifies as

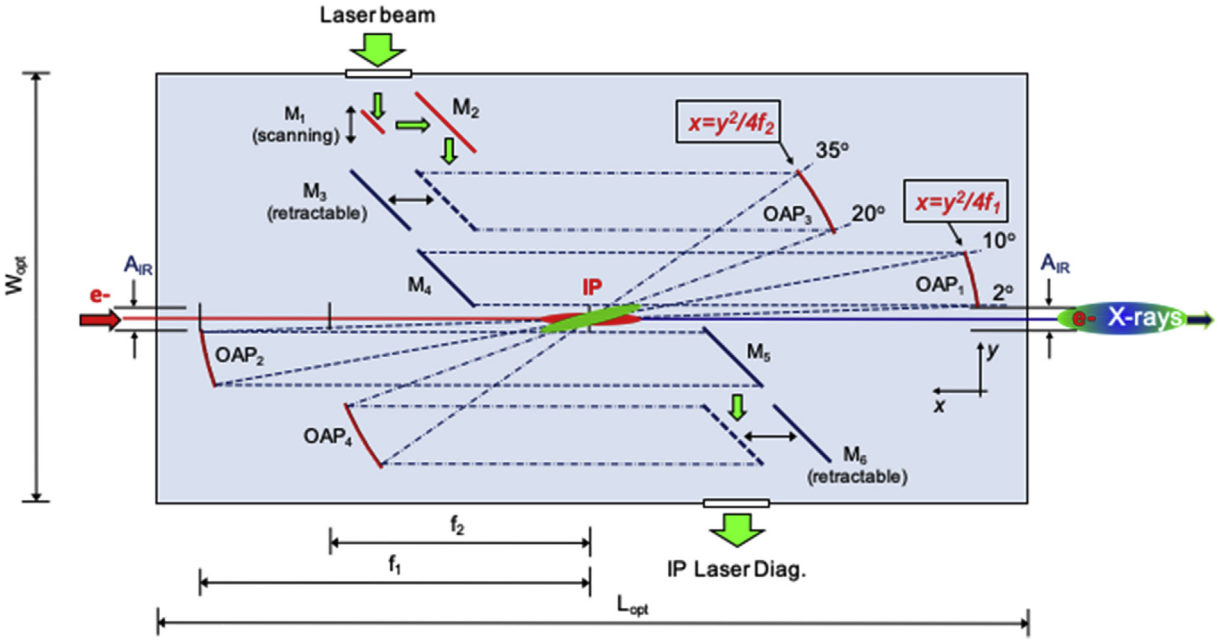

Fig. 8. Proposed layout of the optical box at the BoCXS laser-electron interaction region. A double OAP mirror setup selects the interaction angle ϕ between an operational range $\Delta\phi_1 = 2^\circ - 10^\circ$ (mirrors M_4 – OAP_1) and a larger set $\Delta\phi_2 = 20^\circ - 35^\circ$ (mirrors M_3 – OAP_3) to produce, in combination with small angle operation, X-ray energy shifts of the order of 2–3 keV for KES dual-energy imaging.

$$E_X^{ICS} \cong \frac{2(1+cos\phi)}{1+(\gamma\theta)^2}\, E_{ph}\, \gamma_{ICS}^2. \tag{7}$$

The electron bunches produced in a photo-injector and accelerated in a linac structure have durations 20–30 times shorter than those in synchrotron-based Light Sources and the associated radiation is emitted in much shorter pulses.

In a classic ICS approach, photons are produced by a laser and their energy can be modified by acting on the harmonic of their wavelength. Second harmonic generation (SHG), also referred to as frequency doubling, is a non-linear optical process through which two same-frequency photons interact with a non-linear crystal generating a new photon with twice the energy of the interacting photons. A light pulse undergoing the SHG frequency upshift process will emerge with half the initial photon population and twice the original energy.

With the introduction of the SHG concept the ICS radiation (3) takes the form

$$E_X^{ICS} = \frac{2(1+cos\phi)}{1+(\gamma\theta)^2}\, h_L\, hc\, \frac{\gamma_{ICS}^2}{\lambda_{ph}^0} \tag{8}$$

where $\lambda_{ph} = \lambda_{ph}^0/h_L$ is the actual wavelength of the laser photons and h_L the harmonic (second harmonic: $h_L = 2$).

Adopting the numerical relationships $\gamma = 1.957\, E_e\ (MeV)$ and $hc = 1.24\ eV\ \mu m$ the on-axis scattered photon energy for the fundamental wavelength of Yb-YAG laser photons, $\lambda_{ph}^0 = 1.03\ \mu m$, reads in practical units:

$$E_X^{ICS}(keV) \sim 1.84 \cdot 10^{-2}\, h_L E_e^2(MeV). \tag{8a}$$

In an ICS process characterized by the Thomson cross section $\sigma_T = 0.665\ b$ the radiated flux is given by

$$\dot{N}_X \equiv \sigma_T\, L_{ICS} = \frac{\sigma_T}{A(\phi)}\, \frac{Q}{e}\, \frac{E_L^0}{hc}\, \frac{\lambda_{ph}^0}{h_L^2}\, r \tag{9}$$

where L_{ICS} is the luminosity, $n_{ph} \equiv E_L/E_{ph} = E_L^0/(h_L E_{ph}) = E_L^0\, \lambda_{ph}^0/(hc\, h_L^2)$ is the number of photons in the laser pulse, Q is the electron bunch charge, $n_e = Q/e$ the electron bunch population and r the collision rate.

The interaction area $A(\phi)$ for gaussian bunches colliding at a horizontal interaction angle ϕ

$$A(\phi) = 2\pi\Sigma_y \sqrt{\Sigma_x^2 + \Sigma_z^2 tan^2(\phi/2)} \tag{10}$$

involves the convoluted bunch dimensions

$$\Sigma_{x,y} = \sqrt{w_L^2/4 + \sigma_{ex,y}^2}\ \ and\ \ \Sigma_z = \sqrt{\sigma_{Lz}^2 + \sigma_{ez}^2} \tag{11}$$

where w_L is the laser beam waist and the notations $\sigma_{ex,y,z}$, σ_{Lz} indicate the rms transverse and longitudinal dimensions of the colliding bunches.

In the case of head-on collisions (MuCLS, ThomX, Sec.4) Eq. (10) simplifies as

$$A(\phi = 0) = 2\pi\, \Sigma_x \Sigma_y. \tag{10a}$$

For a given set of the colliding bunch intensities the flux (9) is usually optimized by tuning the interaction area (10) for the best overlap of the colliding bunches, i.e. making their sizes as small and equal as possible.

The expressions (8a) and (9) show that the harmonic h_L of the laser wavelength plays an important role as a multiplier for the radiated energy but also implies a drastic reduction factor for the flux.

Options for controlling the interaction angle ϕ for fine adjustments during operation and to produce controlled energy shifts of about 2–3 keV for two-colour KES experiments (Section 5.1.1) is discussed in Appendix.

2.3. From national/international infrastructure to laboratory X-ray sources

The expressions (2) and (3) for the radiation emitted by the two accelerator-driven sources have similar form and the electron energies required to produce X-ray beams with comparable characteristics are related as

$$E_{ICS} \approx E_U \sqrt{\frac{\lambda_{ph}}{\lambda_u}}\ \sim 10^{-2} E_U \tag{12}$$

where E_U and E_{ICS} are the electron energies in the Undulator and the ICS systems.

The about four orders of magnitude difference between the undulator period ($\lambda_U \sim 15\ mm$) and the laser photon wavelength ($\lambda_{ph} \sim 1\ \mu m$) allows for about two orders of magnitude reduction in the electron energy required in an ICS-based source to produce X-ray beams with the same average energies available at large facilities at a fraction of cost and size. The quadratic dependence of the emitted radiation (3) on the incoming electron energy makes it possible to build an ICS-based X-ray source providing radiation in the multi-100 keV range with electron energies around 100 MeV.

Figs. 4 and 5 provide a comparison between a large national light source like ESRF in Grenoble and a laboratory-size facility like the Compact Light Source (CLS) [8,9] providing X-ray beams within comparable energy ranges.

3. Existing/proposed compact ICS facilities

The flux expression (9) contains the ingredients driving the technical choices for different approaches in the ICS technology i.e. the bunch-by-bunch luminosity and the interaction rate.

In projects like MuCLS [10] and ThomX [11] head-on interactions at relatively low bunch-by-bunch luminosity occur inside a straight pipe in common to a small storage ring and an optical cavity at high frequencies r defined by the ring central path length. The maximum energy of the scattered radiation is in this case defined by the electron energy for which the storage rings are designed.

MuCLS, designed and produced by Lyncean Technologies Inc. (LTI), Palo Alto, California, is presently installed at the TUM (Technical University of Munich). Based on a 4.6 m circumference electron storage ring and a laser-fed optical cavity it provides up to 40 keV X-rays with a peak flux of 3×10^{11} ph/s following a recent upgrade [12]. The Thom-X source involves a 50 (70) MeV, 18 m circumference electron storage ring and a Fabry-Perot laser amplifier resonator. It provides X-ray beams with energies up to 46 (90) keV and an average flux in the 10^{11}–10^{13} ph/s range.

In the STAR [13] and BoCXS designs higher bunch-by-bunch luminosities are produced with much lower repetition rates adopting higher values for the electron bunch charge Q and the laser pulse energy E_L^0. The modularity of a linear accelerating structure not coupled to a storage ring adds flexibility to the electron and the radiated energies for possible upgrades. The STAR system installed at the Calabria University site at Rende, Cosenza, Italy, makes use of a 66 MeV linac and a Yb-YAG laser operated at 0.15 J/pulse, 100 Hz repetition rate. It is designed to produce X-rays featuring a 3×10^9 ph/s average flux at 80 keV maximum energy with the laser operated on the fundamental (1020 nm) harmonic. The proposed BoCXS source, described in the next section, consists, in its base configuration, of an 80 MeV linac providing 120–240 keV tunable X-ray energy in two separate arms to alternatively feed two different user areas. The associated flux corresponding to a 2° interaction angle is (2.0–0.5) x10^{10} ph/s with a Yb-YAG laser operated on the fundamental and second harmonic at 0.85 J/pulse, 100 Hz repetition rate.

Differently from the above-mentioned projects the BriXS (Bright and compact X-ray Source) system [14] is proposed as a twin X-ray ICS source based on two recirculated superconducting 30–100 MeV linacs (SRF

technology) and on a laser system in Fabry-Pérot cavity operated at a100 MHz repetition rate to produce 20–180 keV monochromatic X-rays with an estimated flux of ($5 \times 10^{11} - 3 \times 10^{13}$) ph/s mainly devoted to medical applications. BriXS is designed to be installed in the Expo-Milano area and is presently in the design study phase.

STAR and THOM-X are in the commissioning stage while MuCLS is the only facility operational in Europe and routinely working for about three years in the field of preclinical imaging.

4. The BoCXS proposal

The source BoCXS (**Bo**logna **C**ompact **X**-ray **S**ource) has been conceived as the cornerstone of a Multidisciplinary facility to be realized in the Bologna metropolitan area. The features characterizing a compact ICS-based X-ray source, like high brightness and tunable energy associated to a large degree of monochromaticity would bridge the gap between the commercially available conventional sources and the large and difficult to access Synchrotron light sources.

The proposed facility is derived from the STAR structure and exploits the ICS technology successfully pioneered at the Lyncean Technologies (LTI) premises in Palo Alto and currently operational at the MuCLS facility in Munich. The compact structure is designed to make available X-ray beams with characteristics similar than those available in large Synchrotrons to clinics, universities and research laboratories.

In the base version schematically illustrated in Fig. 6, short electron bunches produced in a Photo-injector are accelerated in a single RF linac structure and transported via independent lines to two optical interaction regions where they interact with intense photon pulses produced by the same laser system operating on the fundamental or its second harmonic. Intense and quasi-monochromatic X-ray pulses are emitted in two different energy bands alternatively feeding two user areas equipped for different applications. The electron linac consists of a 3-m long S-Band structure operating at a tunable 25 MV/m maximum accelerating gradient providing up to 80 MeV electron energy. The Yb-YAG laser system operates with 0.85 J/photon pulses at a 100 Hz repetition rate providing X-ray energies in the (120–240) keV range at the fundamental frequency and its second harmonic. The project makes use of commercially available technologies for which no R&D program is required. Nevertheless, the choice of the S-band technology for the linac accelerating structure is not frozen and could evolve into the C- or even the X-band whenever the state-of-the-art for the structures and the electron guns attains a safe degree of reliability.

The base version of Fig. 6 could, in a further stage, be upgraded following the scheme of Fig. 7, by raising the electron energy up to 155 MeV with the adoption of a second RF accelerating structure. The radiation energy from the upgraded BoCXS version would span one order of magnitude, from below 100 keV to about 1 MeV, considerably broadening the application spectrum of the facility.

The BoCXS expected performance in base (*I*) and upgraded (*II*) configuration is collected in Table 1.

5. Applications

5.1. Biomedical imaging

The unique features of monochromatic X-rays have been proven to be of great interest for medical research and crucial for the implementation of several innovative techniques, mainly in radiology and radiotherapy [15]. Synchrotron Radiation (SR) is the gold-standard for any application requiring high-brilliance monochromatic X-rays, especially in the energy range below 100 keV. Nevertheless, the limited accessibility to monochromatic intense X-ray sources has prevented, so far, the transfer of many diagnostic and therapeutic techniques to clinical routine. A more accessible source would be paramount for preparation of samples and preliminary testing, making possible a quick and flexible transfer of researchers, samples and equipment from the user home laboratory.

ICS-based facilities are among the most promising innovative sources of radiation and many laboratories worldwide are operating or proposing scientific programs to develop and commission this kind of sources. Concerning biomedical applications, experiments on absorption and phase-contrast imaging [16,17], K-edge subtraction techniques and computed micro-tomography on phantom [18], biological [19], animal [20] and human samples [21] with X-rays in the keV range have been already performed. Therefore, the availability of short X-ray pulses in the 30–240 keV energy range delivering about 10^{10} photons/s could pave the way to several pre-clinical applications.

5.1.1. Dual-energy imaging

Generalized subtraction techniques aim at improving lesion conspicuity, defined as the ratio between lesion contrast and surround complexity, which is the ultimate limitation to its detection in diagnostic radiology [22]. Dual-energy imaging could help to enhance the detectability of lesions by removing this “structure noise”. It makes use of two digital images obtained with two different X-ray spectra. The K-Edge digital Subtraction (KES) technique takes advantage of the sharp rise of the absorption coefficient of a contrast agent injected in the tissues to be visualized. This technique is based on the acquisition of two images at energies bracketing the K-edge of the element, ideally with monochromatic X-ray beams. The logarithmic subtraction of the low- and high-energy image enhances the structures filled with the contrast agent, while the signal produced by the other structures is nearly cancelled since their attenuation coefficients are almost identical at the two energies [3]. A recent review concerning the development of the KES techniques and the technology applied to biomedical imaging, from the early low-power X-ray tubes to the latest synchrotron sources, clearly shows that with the advent of new X-ray sources such as compact Compton sources, KES imaging research and potential clinical applications will continue to be important areas of biomedical research [23]. Finally, dual-energy applications have been widely applied for tissue characterization, because they provide a precise and reliable measure of the distribution of a specific tissue within the body [24,25].

5.1.2. Phase-contrast imaging

It is well known that in conventional radiography the contrast is due to the attenuation of X-rays within the sample. In X-ray phase-contrast imaging (XPCI) the mechanism that contributes to the image formation process is generated by the phase shifts imparted to the beam by the sample [26]. Over the years, several studies have clearly demonstrated that phase-contrast can dramatically improve the visibility of details of interest and its potential has been investigated for many applications, including materials science, security, biology, and medicine [27]. Presently, various phase-sensitive techniques have been investigated and tested by means of synchrotron radiation sources, thanks to their unique features to generate high-brilliance and highly coherent X-ray beams. The characteristics of the proposed X-ray source make it particularly suited for techniques which take advantage of the high degree of spatial coherence of Compton source, e.g. propagation-based phase-contrast imaging (PPCI). Since the phase-shift induced in the X-ray beam is not directly detectable, interference phenomena are typically exploited to convert it into an intensity modulation, so as to be recorded by conventional X-ray imaging systems [28]. PPCI relies in the free propagation of the X-beam after the interaction with the sample and does not require additional optical elements. Therefore, it could be easily implemented by simply using a high-resolution X-ray detector located at a suitable distance from the sample.

Furthermore, the possibility to perform XPCI with hard ($\geq$50 keV) X-rays is of particular interest for biomedical applications, since phase shifts effects decrease with increasing energy as $1/E^2$ while absorption effects, responsible for dose deposition, decrease as $1/E^3$. The real part of the refraction index $n = 1 + \alpha + i\beta$ for X-rays is large with respect to the imaginary part. For soft tissues, typical values are $\alpha = 0.3 \times 10^{-6}$ and $\beta = 0.1 \times 10^{-9}$ in the 30–60 KeV range of the X-ray spectrum. As a

consequence, imaging procedures based on phase variation rather absorption techniques are much more efficient especially for such type of tissues. Methods based on interferometry, enhanced diffraction and phase contrast have been developed, but the last one is simpler to implement and widely used in medical imaging [29]. Hard X-ray XPCI could then yield improved image contrast with strongly reduced exposure times and doses.

5.1.3. Animal imaging

Nowadays, translational research plays an essential role in understanding pathophysiology mechanisms of human diseases to develop new diagnostic and therapeutic solutions for their management [30]. Once the animal disease model is created, pathophysiologic changes and effects of a therapeutic treatment are normally studied on the animals via immunohistologic or non-invasive imaging techniques. Animal imaging can be performed by a number of techniques including X-ray computed tomography, magnetic resonance imaging, ultrasound imaging, positron emission tomography, single photon emission computed tomography, fluorescence imaging, and bioluminescence imaging, among others. Individual imaging techniques provide different kinds of information regarding the structure, metabolism, and physiology of the animal. It is for example possible to detect microvessel function in different organ systems of small animals in vivo.

Vascular networks in the brain are poorly understood and represent ideal candidates for imaging studies. SR brain microangiography offers real-time monitoring of microvascular dynamics [31].

Experimental asthma investigations have been carried out to study allergic reactions by using rabbit model. By means of SR-based computed tomography (CT), the simultaneous quantitative imaging of airway structure and regional lung ventilation is obtained with high spatial resolution [32].

Therefore, the expected beam characteristics of the BoCXS source could represent an ideal probe for a number of investigations in preclinical research.

5.1.4. Small-angle X-ray scattering

Coherently scattered X-rays represent an important instrument for characterization of materials. Indeed, position and intensity of the peaks in the scattering pattern reflect the material structure. Two regimes are possible, namely wide and small angle X-ray scattering (WAXS and SAXS), respectively. In particular, the former allows to look at the atomic scale structures, while the second allows to assess the supra-molecular structures and the large-scale arrangement (10–1000 nm) of the material. Several studies in the past years showed that of coherent scatter-based techniques can be used to perform material identification with higher signal-to-noise ratios than is currently possible using X-ray absorption techniques. This fact can be used in a variety of applications, spanning from biology to homeland security. For what concerns medicine, several authors showed that healthy and diseased tissues feature very different scattering patterns, which can then be exploited to make a diagnosis. As an example, the changes in collagen structure when cancer invades connective tissues and the large differences in the SAXS intensity may be used to identify diseased samples [33]. Finally, experimental data, can be used to extract molecular form factors, which are useful for tissue modelling in Monte Carlo simulations [34]. The intense, tunable and monochromatic X-ray beams provided by BoCXS are very well suited to implement the described scattering techniques in an effective way.

5.1.5. Interactive holographic tomography

Volumetric display technology, introduced about 20 years ago, gained momentum in Virtual Reality (VR) and Advanced Visualization (AV) applications before providing a very exciting impact in medical applications with X-ray Digital Tomosynthesis and Holographic 3D Imaging. The Holographic imaging technique collects images obtained from a set of different illumination angles and combines them digitally [35]. The result is a fully interactive holographic light field that can be viewed from any angle, without headgear or special glasses. A digital visual revolution in medicine, 3D Volumetric Technology [36], recently showcased at the Radiological Society of North America (RSNA) conference, brings digital content to life and helps to visualize and communicate in a collaborative way.

5.2. Transient states in condensed matter

For applications in condensed matter physics and related areas (chemistry, biophysics etc.) there are great opportunities for the use of the BoCXS facility as an X-ray source with energy tunable up to 120 keV (initial phase) thanks mainly to the short pulse length (~1 ps) and a 100 Hz repetition rate. In fact, the last 10 years have witnessed a great surge of interest worldwide in time dependent studies of transient states in solids, materials and molecules; the most relevant example is the study of transient states induced by the absorption of visible light, which is a fundamental step in many energy conversion processes in materials, not to mention photosynthesis. Optical laser pump and X-ray probe methods have opened new research areas both using synchrotron radiation (SR) sources and free electron lasers (FELs). The pulse length of BoCXS, in fact, is intermediate between SR (several 100 ps) and FELs (10–100 fs). A pulsed X-ray source with pulse duration <5 ps would allow time-dependent studies using diffraction and absorption methods complementary to those conducted at SR and FEL major facilities. Many physical and chemical processes (e.g. charge carrier diffusion and trapping in materials for light harvesting) occur on the time scales up to several 100 ps, which could be probed by BoCXS. An important characteristic of BoCXS is that both the pump and the probe pulse could be obtained from the same laser, providing jitter-free experiments.

5.3. Non-destructive testing

Non-destructive testing (NDT) is widely used in industry for checking the quality of production, as well as part of routine inspection and maintenance. Among the many possible methods, radiography and ultrasound echography are generally used for the detection of internal flaws located below the surface. Radiographic inspection techniques are frequently used for welds and castings checking and for components inspection. Radiography can also be used to inspect assemblies to check the condition and proper placement of components and of sealed liquid-filled systems. In the case of mechanical and automotive industry most samples are composed by materials with high X-ray attenuation coefficients, such as iron. The use of conventional sources, such as X-ray tubes providing photon energies from a few keV to 300 keV, allows the inspection of iron specimens with thickness up to 7.5 cm. Sources of gamma radiation in the MeV range from isotopes such as Co-60 allow to reach depths of 25 cm. The imaging with X-rays ranging from 100 keV to 0.9 MeV would allow dealing with iron samples with thickness ranging from 2.5 to 20 cm. Two-dimensional radiography or tomographic X-ray imaging of such high-absorption samples, performed with the tunable monochromatic X-ray beams provided by BoCXS coupled to a suitable imaging detector, will be of great interest for mechanical and automotive industry, which is well developed in the neighbouring area.

On the other hand, NDT of samples involving low X-ray absorption or very small details, can take advantage of the phase contrast imaging possibilities enabled by the coherence characteristics of BoCXS X-ray emission.

This is the case of electronic assemblies inspection aimed at detecting cracks, broken wires, missing or misplaced components, taking advantage of the high-resolution and detection low-contrast features capabilities of XPCI.

5.4. Cultural Heritage Science

Non-destructive diagnostics of Cultural Heritage, both for imaging (radiography, microtomography, phase-contrast imaging, …) and

material characterization (XANES, XAS, …), using intense monochromatic beams are well established and widely applied by using synchrotron radiation. The availability of energy-tunable, monochromatic X-ray beams produced in compact sources of moderate cost and limited space requirements, such as BoCXS represents a unique opportunity for the application of this techniques. The possibility to access a closer laboratory or to an "in-situ" installation would definitely facilitate the Cultural Heritage Science.

Furthermore, a unique feature is the possibility to access higher X-ray energies (>100 keV), with respect to those available at synchrotron facilities. This is particularly interesting in many applications, such as Geoarchaeology, which can require the characterization of very small archaeological findings like prehistoric teeth and jewelry, the possibility of deciphering ancient and very fragile manuscripts without opening them, the non-invasive inspection of large artifacts and burial objects wrapped inside soil blocks and other heritage treasures possibly involving considerable sizes. Depending on the nature of the artifacts present inside the soil blocks their tomographic analysis may require highly penetrating X-rays beams in combination with detectors providing high-resolution imaging for this type of radiation.

6. Summary

In the framework of a possible realization of a multidisciplinary facility in the Bologna metropolitan area, conceived to promote cutting-edge technologies for advanced biomedical imaging, we have described the source BoCXS, a Compact X-ray source based on the inverse Compton scattering innovative and demonstrated technology. Thanks to recent impressive progress in the laser technology, ICS-based X-ray facilities, once penalized by the small Thomson cross section, can today bridge the existing gap between conventional, commercially available sources and large Synchrotron facilities in terms of beam characteristics. The outlined proposal aims at providing X-ray beams with characteristics of monochromaticity and brightness comparable to those obtainable al large Synchrotron sources, in a cost-effective way and at a fraction of required space with enhanced availability to users. The accomplishment of this project would represent a remarkable step in the direction of translation of established synchrotron-radiation techniques and implementation of further innovative scientific applications. Although mainly conceived for biomedical diagnostics, the wide range of possible applications in research and industry would confer to this facility a unique multidisciplinary character in Italy.

CRediT authorship contribution statement

A. Bazzani: Conceptualization. **P. Cardarelli:** Writing - review & editing. **G. Paternò:** Investigation, Visualization, Writing - review & editing. **M. Placidi:** Conceptualization, Investigation, Visualization, Writing - original draft, Supervision. **A. Taibi:** Writing - review & editing. **G. Turchetti:** Conceptualization, Supervision.

Declaration of competing interest

The authors declare that they have no known competing financial interests or personal relationships that could have appeared to influence the work reported in this paper.

Acknowledgements

The authors wish to acknowledge valuable and enlightening conversations about the scope and the structure of the workshop with F. Baruffaldi (IRCCS Istituto Ortopedico Rizzoli), F. Boscherini (Department of Physics and Astronomy, Bologna University), M. Gambaccini (Department of Physics and Earth Sciences, Ferrara University) and L. Serafini (INFN-Milan and University of Milan). They are moreover indebted to M.P. Landini (IRCCS Istituto Ortopedico Rizzoli) and F. Palmonari (Department of Physics and Astronomy, Bologna University) for their support and contributions to the successful organization of the workshop.

APPENDIX_A – Controlling the interaction angle

The control of the interaction angle via the kinematic factor (5) represents a useful tool to tune the energy of the emitted radiation [37] both for fine adjustments during operation as well as for producing controlled energy shifts for two-colour KES experiments (Section 5.1.1). The interaction region optical layout proposed in Fig. 8 has been conceived involving the focusing properties of two sets of Off-Axis Parabolic (OAP) [38] mirrors adopting different focal lengths to contain the width of the optical box. The minimum interaction angle $\phi_{min} = 2^o$ and a clearance $A_{IR} = \pm 10$ *mm*required for the ingoing/outgoing e− and X beams at the lower edge of the $OAP_{1,2}$ mirrors, together with a $p\tilde{}1$ *mm* margin between the mirror edge and the laser beam, define the focal length of the $OAP_{1,2}$ mirrors, as

$$f_1 = (A_{IR} + p)/\tan\phi_{min} = 315\ mm. \tag{13}$$

A second set of OAP mirrors ($OAP_{3,4}$, $f_2 = 210$ *mm*) allows for a wider interaction angle range in order to produce, in combination with the $OAP_{1,2}$ mirrors, X-ray energy shifts of the order of 2–3 keV.

The interaction angle ϕ can thus be selected among two ranges, $\Delta\phi_1 = 2^o - 10^o$, $\Delta\phi_2 = 20^o - 35^o$defined by the position of the incoming laser beam onto the mirror M_2, controlled by the scanning mirror M_1.

The operational range $\Delta\phi_1$, selected by the mirror M_4, provides quasi-head-on ICS interactions with fine-tuning options. In addition, the insertion of the retractable mirror M_3 allows selecting the range $\Delta\phi_2$via the mirror OAP_3 to produce, in combination with the small angle nominal operation, X-ray energy shifts of the order of 2–3 keV for KES dual-energy imaging.

A rapid actuation of the position of the $M_{3,6}$ retractable mirrors allows for fast data acquisition across the K-edge of interest. Finally, the mirrors $OAP_{2,4}$ and $M_{5,6}$ recover the laser beam after interaction for diagnostic purposes.

The projected sizes of the OAP mirrors on the plane of Fig. 8 are defined by the intercepts of the interaction angles of interest over the parabolas $y^2 = 4f_{1,2}\,x$.

The main parameters of the optical scheme of Fig. 8 are collected in Table 2.

APPENDIX_B – Preliminary cost estimate

A preliminary cost estimate for the Project options illustrated in Figs. 6 and 7 is presented below.

Phase I – Linac energy ≤80 MeV

Maximum X-ray energy 120 keV, flux $\sim 2 \times 10^{10}$ ph/s.
Maximum X-ray energy 240 keV, flux $\sim 0.5 \times 10^{10}$ ph/s.

S-Band photo-injector	0.5 M€
S-Band cavity (25 MeV/m)	0.2 M€
Klystron	1.0 M€
Yb-YAG Laser (0.8 J/100 Hz rep. rate)	3.5 M€
Diagnostics, beam pipes, magnets	1.0 M€
Integration (clean room, air treatment)	0.8 M€
Controls	1.0 M€
TOTAL	**8.0 M€**

Phase II – Linac energy $\leq$155 MeV

Maximum X-ray energy 440 keV, flux $\sim 2 \times 10^{10}$ ph/s.
Maximum X-ray energy 880 keV, flux $\sim 0.5 \times 10^{10}$ ph/s.

Additional linac module, klystron, beam pipe	**1.5–2.0 M€**

References

[1] C. Pellegrini, A. Marinelli, S. Reiche, The physics of free-electron lasers, Rev. Mod. Phys. 88 (2016), https://doi.org/10.1103/RevModPhys.88.015006.
[2] E. Esarey, S.K. Ride, Ph. Sprangle, Non linear Thomson scattering for Intense laser pulses from beams and plasmas, Phys. Rev. 48–4 (Oct. 1993).
[3] G.A. Krafft, G. Priebe, Compton Sources of Electromagnetic Radiation, in: A.W. Chao, W. Chou (Eds.), Reviews of Accelerator Science and Technology, vol. 3, 2010, pp. 147–163.
[4] C. Sun, Y.K. Wu, Theoretical and simulation studies of characteristics of a Compton light source, PRSTAB 14 (2011), 044701.
[5] A. Curatolo, et al., Analytical Description of Photon Beam Phase Spaces in Inverse Compton Scattering Sources, 22 May 2017, https://doi.org/10.1103/PhysRevAccelBeams.20.080701 arXiv:1705.07740v1 [physics.acc-ph].
[6] N. Ranjan, et al., Simulation of inverse Compton scattering and its implications on the scattered linewidth, PRAB 21 (2018), 030701, https://doi.org/10.1103/PhysRevAccelBeams.21.030701.
[7] G. Paternó, et al., Inverse Compton radiation: a novel x-ray source for K-edge subtraction angiography? Phys. Med. Biol. 64 (2019) 185002, 17pp).
[8] CLS –. https://journals.aps.org/prl/abstract/10.1103/PhysRevLett.80.976.
[9] B. Hornberger, et al., A compact light source providing high-flux, quasi-monochromatic, tunable X-rays in the laboratory, in: Proc. SPIE Optical Engineering + Applications, 2019. San Diego, California, United States SPIEDigitalLibrary.org/conference-proceedings-of-spie.
[10] F. Pfeiffer, et al., doi:10.1038/nphys265,26_March_2006.
[11] ThomX. https://thomx.lal.in2p3.fr/.
[12] Lyncean Technologies Inc, White Paper, Jan. 2019.
[13] STAR Project – Proc. IPAC2014, Dresden, Germany.
[14] I. Drebot, et al., BriXS ultra high flux inverse Compton source based on modified push-pull energy recovery linacs, Instruments 3 (2019) 49, https://doi.org/10.3390/instruments3030049,10_September_2019.
[15] F.E. Carroll, Tunable monochromatic X rays: a new paradigm in medicine, Am. J. Roentgenol. 179 (2002) 583–590.
[16] H. Ikeura-Sekiguchi, et al., In-line phase-contrast imaging of a biological specimen using a compact laser-Compton scattering-based x-ray source, Appl. Phys. Lett. 92 (2008) 131107.
[17] R. Gradl, et al., Propagation-based phase-contrast X-ray imaging at a compact light source, Sci. Rep. 7 (2017) 4908.
[18] K. Achterhold, et al., Monochromatic computed tomography with a compact laser-driven X-ray source, Sci. Rep. 3 (2013) 1313.
[19] M. Bech, et al., Hard X-ray phase-contrast imaging with the compact light source based on inverse Compton X-rays, J Synchrotron radiation 16 (2009) 43–47.
[20] F.G. Meinel, et al., Diagnosing and mapping pulmonary emphysema on X-ray projection images: incremental value of grating-based X-ray dark-field imaging, PloS One 8 (2013), e59526.
[21] E. Eggl, et al., X-ray phase-contrast tomosynthesis of a human ex vivo breast slice with an inverse Compton x-ray source, Europhys. Lett. 116 (2017) 68003.
[22] A. Taibi, Generalized subtraction methods in digital mammography, Eur. J. Radiol. 72 (2009) 447–453.
[23] W. Thomlinson, et al., K-edge subtraction synchrotron X-ray imaging in bio-medical research, Phys. Med. 49 (2018) 58–76.
[24] P. Vock, Z. Szucs-Farkas, Dual energy subtraction: principles and clinical applications, EJR (Eur. J. Radiol.) 72 (2009) 231–237.
[25] T.P. Szczykutowicz, Dual-energy and spectral imaging, in: A. Brahme (Ed.), Comprehensive Biomedical Physics, vol. 2, Elsevier, Amsterdam, 2014, pp. 155–166.
[26] L. Rigon, X-ray imaging with coherent sources, in: A. Brahme (Ed.), Comprehensive Biomedical Physics, vol. 2, Elsevier, Amsterdam, 2014, pp. 193–220.
[27] P. Bravin, et al., X-ray phase-contrast imaging: from pre-clinical applications towards clinics, Phys. Med. Biol. 58 (2012) 1. R1.
[28] E. Castelli, et al., Mammography with synchrotron radiation: first clinical experience with phase-detection technique, Radiology 259 (2011) 684–694.
[29] M. Endrizzi, X-ray phase-contrast imaging, Nucl. Instrum. Methods A 878 (2018) 88–98.
[30] G.S. Sandhu, et al., Whole animal imaging, Wiley Interdiscip Rev Syst Biol Med. 2 (2010) 398–421.
[31] M. Zhang, et al., Synchrotron radiation imaging is a powerful tool to image brain microvasculature, Med. Phys. 41 (2014).
[32] S. Bayat, et al., Methacholine and ovalbumin challenges assessed by forced oscillations and synchrotron, lung imaging, Am. J. Respir. Crit. Care Med. 180 (2009) 296–303.
[33] M. Fernandez, et al., Small-angle x-ray scattering studies of human breast tissue samples, Phys. Med. Biol. 47 (2002) 577–592.
[34] G. Paternò, et al., Geant4 implementation of inter-atomic interference effect in small-angle coherent X-ray scattering for materials of medical interest, Phys. Med. 51 (2018) 64–70.
[35] B. Rymuza, et al., Holographic imaging during transcatheter aortic valve implantation procedure in bicuspid aortic valve stenosis, Kardiol. Pol. 75 (10) (2017) 1056, https://doi.org/10.5603/KP.2017.0195.
[36] https://voxon.co/.
[37] I. Drebot, V. Petrillo, L. Serafini, Two-colour X-gamma ray inverse Compton back-scattering source, Europhys. Lett. 120 (2017) 14002, https://doi.org/10.1209/0295-5075/120/14002.
[38] https://www.edmundoptics.com/knowledge-center/application-notes/optics/off-axis-parabolic-mirror-selection-guide/.